PCCP

Accepted Manuscript

ROYAL SOCIETY OF CHEMISTRY

www.rsc.org/pccp

ARTICLE TYPE www. rsc.org/xxxxxx | XXXXXXXX

Vibrational Spectroscopy of Methyl benzoate

Kiran Sankar Maiti†

Received Xth XXXXXXXXXX 20XX, Accepted Xth XXXXXXXXX 20XX
First published on the web Xth XXXXXXXXXX 200X
DOI: 10.1039/b000000x

Methyl benzoate is studied as a model compound for the development of new IR pulse schemes with possible applicability to biomolecules. Anharmonic vibrational modes of Methyl benzoate are calculated on different level (MP2, SCS, CCSD(T) with varying basis sets) ab-initio PESs using the vibrational self-consistent field (VSCF) method and its correlation corrected extensions. Dual level schemes, combining different quantum chemical methods for diagonal and coupling potentials, are systematically studied and applied successfully to reduce the computational cost. Isotopic substitution of β-hydrogen by deuterium is studied to obtain a better understanding of the molecular vibrational coupling topology.

1 Introduction

Vibrational spectroscopy is among the foremost experimental tools in the exploration of molecular potential-energy surfaces (PES)[1]. Its application to biological systems has so far been severely handicapped, both by experimental difficulties and by the unavailability of adequate computational tools for quantitative interpretation. Several one-dimensional vibrational techniques have been developed for structural determination of the biological molecules. Among them vibrational circular dichroism (VCD)[2,3], Raman optical activity (ROA)[4–6] are two well established polarization techniques. Recent success in the experimental realization of coherent multidimensional infra-red (IR) spectroscopy provides a new powerful tool to study structure and dynamics of biomolecules with a temporal resolution down to the sub-picosecond regime[7–12]. Multidimensional IR spectroscopy has the potential to disentangle the congested vibrational spectra of biomolecules to some extent similar to multidimensional NMR[13,14] but with significantly higher temporal resolution[15]. In nonlinear multidimensional spectra, the structural as well as dynamical information is typically available in terms of diagonal and cross-peak shapes, locations, intensities and their respective temporal evolution[16]. The interpretation of this data in terms of a dynamical model of the biomolecule under investigation requires extensive theoretical modeling.

The calculation of vibrational spectra within the harmonic approximation is very useful, but often has limited significance since many biologically relevant molecules are "floppy" and subject to strong anharmonic effects[17]. Anharmonic effects are even much larger in weakly bound molecular complexes, e.g. hydrogen-bonded complexes with surrounding water[18]. Also, frequently one is interested in the regions of the PES far away from the equilibrium configuration, where the harmonic approximation is even less applicable. The main problem of anharmonic spectroscopic calculations is that different vibrational modes are not mutually separable like in the harmonic approximation[19,20]. Therefore one has to face the task of calculating wavefunctions and energy levels for systems of many coupled degrees of freedom. Several attempts have been made to overcome this problem. Among others, the discrete variable representation (DVR)[21–23], diffusion quantum Monte Carlo (DQMC)[24–26], vibrational configuration interaction (CI)[27–29], vibrational self-consistent field (VSCF)[30–33] methods proved their applicability to study anharmonic effects in systems with varying sizes. The VSCF method is most successful among them to effectively handle large molecular systems.

IR absorption spectra of peptides and proteins are dominated by vibrational bands that can be described approximately in terms of oscillators localized in each repetitive unit and their mutual couplings. The most extensively studied bands are amide-A, amide-B in the region 3000–3500 cm^{-1} and amide-I, amide-II between 1500-1700 cm^{-1}, which are spectrally well separated from the remaining spectrum and exhibit a strong dependence on the structural motifs present in the investigated biomolecules[34,35]. The amide-I vibrational mode, which involves mainly the C=O stretch coordinate, has experimentally been the most important mode due to its large transition-dipole moment and because it appears to be mostly decoupled from the remaining vibrational modes in proteins. A detail understanding of these modes is then necessary to understand the structure and dynamics of the protein and peptide. Due to the complex structure of proteins a detailed theoretical calculation of these modes is complicated. A simple small molecule is then necessary for which these exemplary modes and their mutual couplings can be studied in more detail.

In this work Methyl benzoate (MB) was chosen as a model

† *Physikalische Chemie, Universität Bayreuth, Universitätsstraße 30, D-95447 Bayreuth, Germany. E-mail: kiran.maiti@ch.tum.de*

for potential vibrational couplings between the carbonyl group and a sidechain C-H moiety, which would allow for a determination of backbone-sidechain dynamics in peptides and proteins. MB has an idealized planar configuration, except for the two hydrogen atoms at the methyl group which are symmetrically out-of-plane with respect to the rest of the molecule (see Fig. 1). The methyl carboxylate group is then co-planar with the phenyl ring. The C=O double bond in the carboxylic ester group essentially constitutes a local oscillator similar to the amide-I band in proteins and provides a convenient mode for model studies. A potentially interesting coupling in proteins is the coupling between the amide-I and a β-hydrogen located in the sidechain. MB also provides a similar structural motif where the ortho hydrogen in the phenyl ring provides the counter-part of a β-hydrogen in protein sidechains. The structural similarities of these two motifs in MB and proteins are depicted in Fig. 1b.

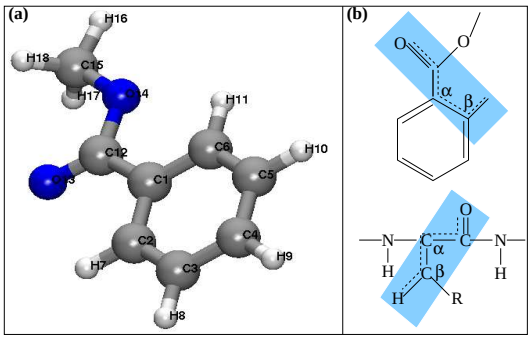

Fig. 1 (a) Structure of MB, indicating the numbering scheme used in this work. (b) Structural similarity of protein backbone and MB.

Isotopic substitution is a valuable tool in the identification of molecular structure and dynamics. The C–H or C–D stretch vibrations are particularly important structural probes, because they are very localized, specific, and abundant. Especially the C–D stretching frequency is an excellent structural probe since it is usually spectrally isolated ($\sim$2200 cm^{-1}) even in the spectrum of large proteins. Substitution of β-hydrogen by deuterium provides a probe to obtain a better understanding of the structure and dynamics of protein sidechains with respect to the backbone. It is thus an interesting task to devise new experiments which probe this relative geometry. MB is an ideal candidate model which, once its vibrational hamiltonian is fully understood, will serve to develop new pulse sequences.

2 Computational methods

2.1 Quantum Chemistry

Geometry optimization of MB has been performed using second order Møller-Plesset[36] (MP2) perturbation theory[37,38] and employing the augmented correlation-consistent polarized-valence-triple zeta (aug-cc-pVTZ) basis set. Harmonic normal-mode analysis has been performed with the density fitting MP2 (DF-MP2) method using an aug-cc-pVTZ regular basis and cc-pVTZ fitting basis sets. All calculations have been done with the MOLPRO quantum chemistry program[39].

The choice of the computational method and the basis set are not arbitrary. A standard MP2 with aug-cc-pVTZ basis set level of computation is generally a reliable method to generate an anharmonic PES. For a system like MB it is not suitable due to the size of the molecule and the resulting high computational cost. To find a suitable method a comparison of computations employing different basis sets has been performed and is presented in Table 1. The standard MP2 calculation employing an aug-cc-pVTZ basis set is given in the first row which provides the reference. To study all 48 modes of MB with this basis set is beyond the scope of this project, because it takes almost one day and a very large memory space for a single-point energy calculation. If no specially optimized fitting basis sets are available for a certain regular AO basis, then it is a common practice for the DF-MP2 computations to use a fitting basis set one order higher than the regular one. The DF-MP2 with aug-cc-pVTZ regular basis and cc-pVQZ fitting basis speeds up the calculation drastically (see Table 1) without sacrificing the quality compared to the standard MP2/aug-cc-pVTZ results. A single-point energy calculation with this method takes only around one and half hour with almost 200 times less memory than regular MP2/aug-cc-pVTZ calculation. In contrast, the DF-MP2 method employing aug-cc-pVTZ regular and cc-pVTZ fitting basis sets gives almost identical energy values in half the time which is a reasonable choice for the purpose of this project. The anharmonic pair couplings are calculated with the DF-MP2 method

Table 1 Single point energy, calculation time and the required memory for energy calculation of MB at equilibrium geometry with different basis sets.

Basis		Energy in E_h			CPU time	Memory
mp2fit	jkfit	SCF	MP2	Total	in min.	in MB
		-457.51	-1.76	-459.27	1423	6799.4
avtz	vtz	-457.51	-1.76	-459.27	47	270.4
avtz	vqz	-457.51	-1.76	-459.27	97	361.7
avqz	vqz	-457.54	-1.86	-459.40	286	3194.9
avqz	v5z	-457.54	-1.86	-459.40	484	3194.9

employing the same cc-pVDZ basis for regular and fitting basis set. For some of the most problematic modes the diagonal potentials have been calculated with the local density fitting coupled cluster singles, doubles and perturbative triple correction DF-L-CCSD(T)[40–42] method with the cc-pVTZ basis set in a dual-level scheme. All computations have been additionally performed using the density fitting spin-component scaled (DF-SCS) MP2 method[43] employing different basis sets.

2.2 Grid for VSCF

The choice of an appropriate grid size is crucial for anharmonic frequency calculations both for diagonal and pair potentials.[44] The VSCF PES can be expressed in terms of a hierarchical expansion

$$\begin{aligned} V(q_1,\cdots,q_N) &= \sum_{j}^{N} V_j^{(1)}(q_j) + \sum_{i<j} V_{i,j}^{(2)}(q_i,q_j) \\ &+ \sum_{i<j<k} V_{i,j,k}^{(3)}(q_i,q_j,q_k) + \cdots \\ &+ \sum_{i<j\cdots<r<s} V_{i,j,\cdots,r,s}^{(n)}(q_i,q_j,\cdots,q_r,q_s) + \cdot \quad (1) \end{aligned}$$

where $V_j^{(1)}(q_j)$ is the diagonal potential, $V_{i,j}^{(2)}(q_i,q_j)$ is the pairwise potential, $V_{i,j,k}^{(3)}(q_i,q_j,q_k)$ is the triple coupling and so on.

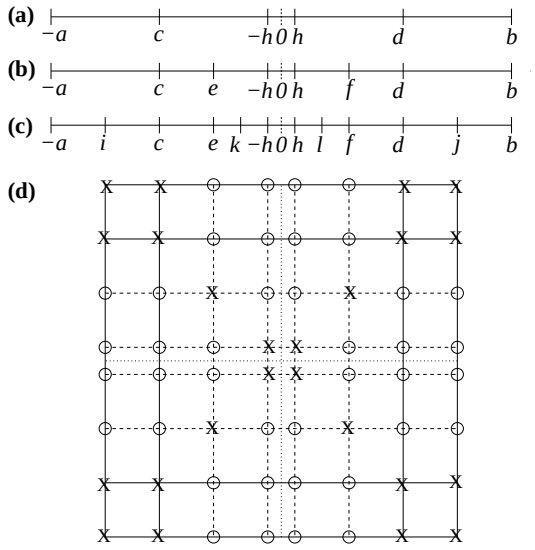

Fig. 2 Diagonal grid with different grid size; (a) 6 points grid, (b) 8 points grid, (c) 12 points grid. (d) Irregular spaced 2D grid. Energy points are calculated at the grids, marked with crosses. The grids marked with circles are filled up by 2D IMLS interpolation.

The grid is constructed based on the harmonic frequency analysis and PM3 PES cuts. The innermost two points (-h, h) are determined from the second derivative of the PES at equilibrium corresponding to the harmonic frequencies of the normal modes. The outer two points (-a, b) are determined as those points on the one dimensional (1D) PES cuts along the normal modes for which the PM3 energy reaches six times the harmonic frequency quantum w.r.t. the energy at equilibrium (V_0). The remaining points are calculated dividing the interval with different proportions e.g., $c = \frac{-a+(-h)}{2}$, $d = \frac{b+h}{2}$, $e = \frac{c+(-h)}{2}$, $f = \frac{d+h}{2}$, $i = \frac{-a+c}{2}$, $j = \frac{d+b}{2}$, $k = \frac{e+(-h)}{2}$ and $l = \frac{f+h}{2}$. Diagonal potentials with 6 points (see Fig. 2a) are insufficient for a reasonable description of the PES in the calculation of anharmonic frequencies. In particular, a denser set of grid points is required near the equilibrium configuration. A comparative study on 8 point (see Fig. 2b) and 12 point (see Fig. 2c) 1D grids indicates that the eight point grid PES is a reasonable choice for anharmonic frequency calculations.

All diagonal points are first evaluated on an 8 point 1D grid as shown in Fig. 2b, then interpolated to equidistant 16 point grids which are used in the collocation treatment. Pair potentials, calculated at semiempirical PM3 level, are evaluated on 8×8 point direct product grids, then interpolated to 16×16 point grids by two-dimensional (2D) cubic spline interpolation[45]. To lower the computational cost while maintaining high quality pair potentials, DF-MP2/cc-pVDZ computations have been performed for selected coupling potentials on irregularly spaced 2D grids, as shown in Fig. 2d. Energies are only calculated for the grid points marked with crosses. The undetermined points (marked with circles in Fig. 2d) are filled with non-uniform IMLS (interpolating moving list-squares)[46] interpolation, which provides a potential on 8×8 point direct product grids. The 8×8 point grid is extended to the 16×16 point grid by using 2D cubic-spline interpolation[45].

3 Results and Discussion

3.1 Vibrational spectrum of Methyl benzoate

To my knowledge, only few experimental results[47] are available for MB. Specially for low frequencies and near degenerate modes all the modes are not well resolved and identified experimentally. Therefore the best computational result, which agrees comparatively well with the known experimental results[47–50], has been choosen as a reference, then discuss all other levels of computation with respect to that. For this purpose, the non-correlated VSCF results are chosen as a reference, where diagonal and pair potentials are calculated using the DF-SCS method employing a cc-pVDZ basis set. All the results presented in this article are with out applying any scaling factors.

The entire vibrational spectrum of MB can be divided into three different frequency regions. Most interesting high fre-

Table 2 Vibrational frequencies of MB with different level of theories, where diagonal grids are calculated with the DF-MP2/AVTZ level. Mode numbers are based on normal mode frequencies. The RMSD calculated with respect to the anharmonic frequency calculated with VSCF/DF-SCS method. The modes for which diagonal anharmonicities are larger than 10 cm^{-1} are with bold numbers.

Mode	Harmonic	Diagonal	VSCF		VC-MP2	VSCF/	Experiment[47]	Isotopomer		Assignment*
			PM3	MP2		DF-SCS		D_7	D_{11}	
1	52	82	147	103	87	112		111	111	Phenyl-ester opr
2	112	154	178	192	160	196		197	198	Phenyl opb, ester opb
3	185	361	366	316	352	342		344	343	CH_3 asb
4	167	170	169	173	169	179	134	177	177	Phenyl-ester ipr
5	208	217	236	239	234	242	218	243	242	Phenyl-ester opb
6	331	333	326	334	331	340		339	340	Phenyl-Ester ipr
7	358	358	356	366	365	363	360	361	361	O=C-O ipb, phenyl ipb
8	404	411	419	416	414	421		402	403	phenyl opb
9	454	458	477	470	466	468		458	461	phenyl opb, O=C-O-C opb
10	481	481	481	476	475	477		474	471	phenyl ipr, O=C-O-C ipr
11	617	617	618	612	611	617	630	612	612	phenyl ipd
12	678	679	685	676	673	681	674	678	680	phenyl ipd O=C-O ipb
13	712	728	788	737	726	754		708	704	phenyl opd O=C-O opb
14	795	801	840	808	837	813	782	829	834	phenyl opd O=C-O opb
15	831	830	818	818	812	823	820	822	821	O=C-O ipb, phenyl, CH_3 ip
16	694	760	759	781	724	731	714	734	725	phenyl opd
17	863	894	880	856	841	891	864			phenyl opr
18	1003	1004	1170	974	971	978		759	771	phenyl ipd, ester ipd
19	1012	1012	1052	991	989	979		973	973	phenyl ipd
20	1048	1049	1146	1029	1025	1035	1027			phenyl ipd, P-CH sipb
21	977	1000	980	978	987	986	980	984	984	phenyl opd, P-CH opb
22	1097	1101	1162	1082	1074	1096	1097	1047	1048	phenyl ipd, P-CH ipb
23	938	970	951	931	926	958	950	956	980	phenyl opd, P-CH opb
24	1142	1144	1220	1111	1103	1126	1128	1112	1121	OCH_3 r, O=C-O ipb
25	1174	1189	1154	1153	1146	1167	1161	1171	1173	pCH ipb
26	1185	1199	1074	1170	1161	1182		1180	1181	CH_3 sopb, C-O-C opb
27	1191	1198	1176	1164	1156	1183	1177	1149	1141	pCH sipb
28	958	994	908	968	982	979		969	984	pCH opb
29	1221	1227	1164	1200	1194	1214	1192	1212	1213	OCH_3 r, O=C s, C-O s
30	1317	1321	1350	1283	1262	1303	1278	1298	1307	OCO ipb pCH ipb
31	1330	1334	1287	1301	1309	1320	1295	1268	1259	pCH ipb
32	1472	1469	1318	1423	1415	1342	1310	1444	1447	CH_3 asb
33	1479	1482	1354	1433	1411	1447	1435	1348	1345	pCC s
34	1471	1475	1461	1436	1434	1452	1444	1445	1455	pCC s
35	1509	1507	1320	1459	1454	1453		1454	1453	CH_3 wagging
36	1519	1517	1322	1488	1488	1485		1485	1485	CH_3 sb
37	1518	1519	1529	1478	1477	1498	1474	1480	1483	pCC s, pCH ipb
38	1634	1636	1750	1587	1581	1606	1594	1602	1600	phenyl ipd-sy
39	1634	1634	1747	1587	1580	1603	1585	1598	1604	phenyl ipd-sy
40	1766	1759	1915	1724	1724	1778	1724	1724	1724	C=O s
41	3092	3059	2909	2946	2795	2974	2998	2974	2973	mCH ss
42	3183	3255	2787	2582	2492	2560	2542	2561	2559	mCH as
43	3205	3208	2887	2893	2849	2855	2855	2809	2889	pCH as
44	3214	3247	2867	2872	2834	2834	2852	2171	2971	pCH as/pCD_7 as
45	3217	3213	2868	2860	2694	2832	2845	2858	2832	mCH ss
46	3222	3233	2913	2995	2849	2963	2952	2831	2957	pCH as
47	3226	3191	2932	3014	3035	3039	3064	3017	3065	pCH as
48	3238	3161	2898	2933	2928	2985	3022	2989	2161	pCH as/pCD_{11} as
RMSD	148	151	78	24	45					

Symbols: R = rotation, r = rocking, ipr = in-plane rotation, opr = out-of-plane rotation, ipb = in-plane bending, opb = out-of-plane bending, ipd = in-plane deformation, opd = out-of-plane deformation, as = asymmetric stretch, ss = symmetric stretch, asb = asymmetric bending, sb = symmetric bending, sipb = symmetric in plane bending, mCH = methyl CH bond, pCH = phenyl CH bond, sy = symmetric.

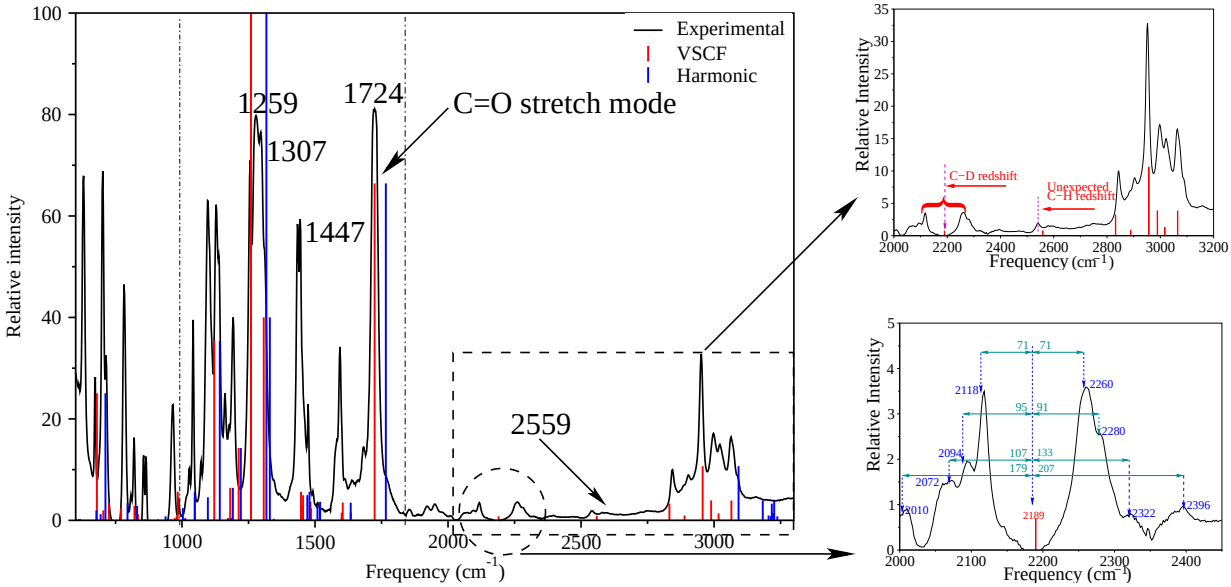

Fig. 3 1D IR experimental spectrum[51] (black line) of deuterated MB is plotted along with calculated harmonic (blue sticks) and anharmonic (red sticks) vibrational frequencies. Intensity of the calculated frequencies are from harmonic frequencies calculation.

quency modes are due to the C-H stretching modes. Low frequency (up to ∼1000 cm^{-1}) modes are primarily due to the bending motions, involving the phenyl ring and the ester group. Between these two extremes, there are modes with combinations of bending and stretching motions and also the spectroscopically well-separated C=O band at about 1725 cm^{-1}.

The vibrational frequencies of all modes of MB calculated at different levels of theory, along with their experimental results and full assignment of all modes are presented in Table 2. FTIR spectra of deuterated MB along with the calculated frequencies are plotted in Fig. 3. The deviation of the vibrational frequencies calculated at different levels of theory w.r.t. the frequency obtained from the non-correlated VSCF/DF-SCS method are plotted in Figs. 4a, 4b and 4c. The harmonic and diagonal anharmonic frequencies are quite off from the reference (VSCF/DF-SCS) frequencies and as a results gives a very high root mean squared deviation (RMSD) of 148 cm^{-1} and 151 cm^{-1} respectively. Addition of PM3 pair coupling potential over DF-MP2/cc-pVDZ diagonal potential improve the results but still with high RMSD value of (78 cm^{-1}). The dual level non-correlated VSCF frequencies with DF-MP2/aug-cc-pVDZ diagonal and DF-MP2/cc-pVDZ pair potentials shows very good agreement with reference frequencies and yield the RMSD of 24 cm^{-1}.

For low frequency modes dual level calculations with PM3 pair couplings are not reliable. The RMSD calculated for all 40 low frequency modes is thus quite high, 73 cm^{-1}. Har-

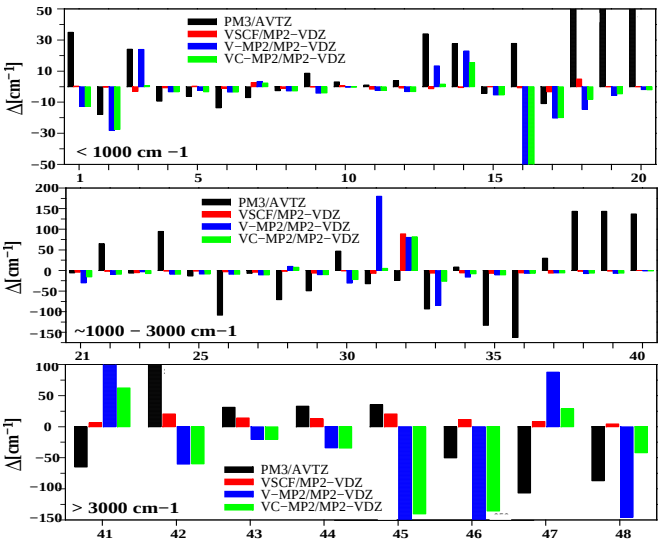

Fig. 4 A comparison of vibrational frequencies of MB calculated at different levels of theory w.r.t. the VSCF/DF-SCS level of calculation. The labels indicate the level of theory used for the calculation. V-MP2 stand for vibrational MP2 and VC-MP2 stand for vibrational corrected MP2.

monic and diagonal frequencies (frequency calculated from the anharmonic diagonal PES) are also quite off for several modes (1, 2, 3, 13, 18, 35, 41 to 48) from the reference frequencies and give RMSDs of 35 cm^{-1} and 37 cm^{-1}, respec-

tively. Frequencies calculated with the non-correlated VSCF method with DF-MP2/cc-pVDZ diagonals and pair coupling potentials are in good agreement with the experimental results, which yields a very low RMSD of 14 cm^{-1} for the 40 low frequency modes. Dual level calculations using DF-MP2/aug-cc-pVTZ diagonal and DF-MP2/cc-pVDZ pair potentials, improve the results further, with a RMSD of 11 cm^{-1}.

3.2 High frequency vibrational modes

The high-frequency vibrational modes (41 to 48) are spectrally isolated from all other modes of MB. The deviation of frequency for these eight modes calculated at different levels of theory w.r.t. the VSCF/SCS-VDZ method is plotted in Fig. 4c. Harmonic and diagonal frequencies are too high (see Table 2). The RMSD only for the C–H stretch vibrational modes (41 to 48) is 319 cm^{-1} for the harmonic frequency, and 454 cm^{-1} for the diagonal frequencies. The large RMSDs for these eight modes from the harmonic and the diagonal frequency calculations are mostly due to the mode 42, which shows an unexpected red shift to the frequency $\sim$ 2550 cm^{-1} (this is discussed in details later). However, when pair couplings are included, the RMSD is reduced dramatically. Dual level calculations, with DF-MP2/aug-cc-pVTZ diagonal potentials and PM3 pair potentials (see Table 2) yield a RMSD of 100 cm^{-1}. Dual level non-correlated VSCF computation with DF-MP2/aug-cc-pVTZ diagonal and DF-MP2/cc-pVDZ pair potentials are surprisingly accurate for the C–H stretch vibrational frequencies. The RMSD calculated for these eight modes is 13 cm^{-1} only.

A rather surprising result of the anharmonic pair-coupling calculations is that one of the C–H stretch vibrational modes is shifted to a much lower frequency than the remaining C–H stretch vibrations. This red shift of the C–H stretch vibrational mode has not been discussed in literature, so far. However, a close investigation of the experimental spectra[52] reveals the presence of an unassigned peak at 2560 cm^{-1} with low intensity. In a recent 1D IR experimental study of deuterated MB by Steinel group[53], a low intensity peak is observed at 2542 cm^{-1} which matches with the calculated frequency (see Fig. 3).

Closer inspection of this mode reveals that this frequency originates from the combination of anti- symmetric C–H (two out of plane hydrogens) stretch vibration in the methyl group along with the out of plane rotation of the ester group w.r.t. the phenyl ring about the C–C bond (mode 1). The ester group rotational motion pulls in one out-of-plane hydrogen to the plane of molecule and pushes the other from the molecular plane (see Fig. 5a). Such a bi-directional force changes the force constant of the anti- symmetric C–H stretch vibration, which unexpectedly lower the vibrational frequency of this band. Since this vibrational mode (mode 42) is strongly coupled with the lower frequency mode 1, the harmonic and the diagonal anharmonic analysis fails to describe it, where as pair coupling analysis explain it.

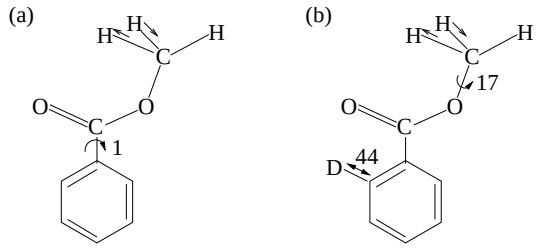

Fig. 5 (a) Vibrational motion of MB responsible for the unexpected red shift. (b) Secondary coupling of C–D and rotational methyl group.

3.3 C=O band

The spectroscopically most studied vibrational band in peptides is the amide-I band. In the MB spectrum the C=O stretch vibrational band which is analogous to amide-I band, is spectrally isolated from all other vibrational frequencies. The harmonic and the anharmonic diagonal frequencies of the C=O stretch vibration at DF-MP2/aug-cc-pVTZ level are relatively high (1766 cm^{-1} and 1759 cm^{-1} respectively) for this mode, compared to its experimental frequency (1724 cm^{-1}) (see Table 2). Dual level frequency calculations employing DF-MP2/aug-cc-pVTZ diagonal and the PM3 pair potential is even worse (see Table 2). The calculated C=O frequency is improved when dual level calculations are performed replacing the DF-MP2/cc-pVDZ diagonal potential for the C=O vibrational mode alone by a DF-L-CCSD(T)/cc-pVTZ diagonal potential. A perfect match is obtained with the experimentally observed frequency (1724 cm^{-1}). For the C=O stretch mode a high level description of the diagonal potential is thus of tantamount importance.

4 Deuterated Methyl benzoate

Deuteration of MB in the ortho position of the benzene ring yields the syn- and anti- isomers of ortho-deutero methyl benzoate (o-DMB) shown in Fig. 6. In the potential energy minima the ester group remains in the same plane as the benzene ring. Upon thermal excitation, the conformers interconvert by a rotation of the ester group around the C–C bond axis. The barrier height for the ester group rotation in MB is estimated at $\sim$ 0.25 eV, as calculated by the DF-MP2 method with aug-cc-pVTZ basis set. This is rather small and easily accessible even at room temperature and thus the conformers can easily interconverted. Although both conformers have nearly the

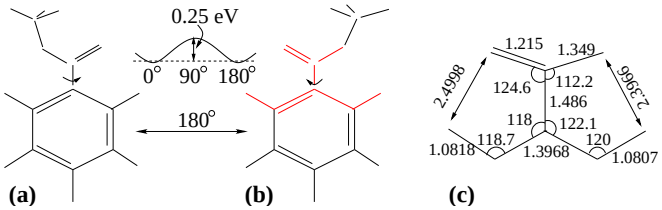

Fig. 6 Two structural conformers of MB and their approximate interconversion barrier height. (a) syn-o-deutero-methyl-benzoate (syn-o-DMB) (b) anti-o-deutero-methyl-benzoate (anti-o-DMB). (c) Possibility to form five member rings between ortho hydrogen of the phenyl ring and the ester group. Bond lengths are given in Å and bond angles in degree.

same molecular energy, they possess different vibrational C–D frequencies due to the different couplings to the ester group. With the best possible computation (dual level VSCF) a C–D stretch frequency difference of about 10 cm^{-1} is found for these two conformers .

4.1 Identification of isotope effects by co-diagonalization

The co-diagonalization[54] method finds a convenient application in vibrational spectroscopy to identify the coupling of different modes and isotope effects. When an atom is substituted with its isotope, some of the eigen vectors differ from the non-substituted molecule. In co-diagonalization these are identified by non-zero off-diagonal elements. The frequency shift for the primary isotope effect appears in the diagonal element and secondary effects appear as off-diagonal elements. Fig. 7 (a) and (b) depict the resulting co-diagonalized matrices of the syn- and anti-o-DMB. In both of the figures, fundamental frequencies are plotted on the diagonal and residual couplings are shown as off-diagonal elements. The diagonal and the upper left triangles are in same scale, shown in the left rainbow colour spectrum. Ten times magnified coupling elements are shown in the lower right triangles, corresponding scale is given on the right side.

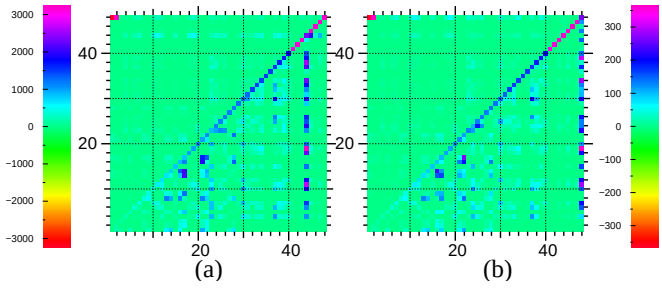

Fig. 7 Frequency spectra (in cm^{-1}) of Methyl benzoate isotopomers. (a) syn-o-DMB and (b) anti-o-DMB.

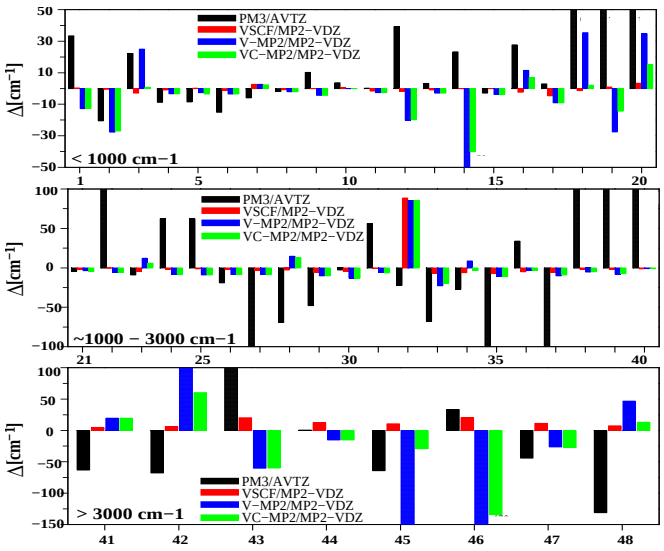

Fig. 8 A comparison of vibrational frequencies of anti-o-DMB calculated at different levels of theory w.r.t. VSCF/DF-SCS level of calculation. The labels indicate the level of the theory used for the calculations.

The syn- and anti-isomers show a clear primary isotope effect for the 44^{th} (2171 cm^{-1}) and 48^{th} (2161 cm^{-1}) vibrational modes, respectively. The secondary isotope effects are mainly due to the coupling with the C–D vibrational mode. A noticeable feature of the isotope effect is that both isotopomers show secondary isotope effects for the same normal modes (modes 8, 13, 14, 17, 18, 19, 20, 23, 27 and 31), where as primary isotope effects are observed for different normal modes. A strong secondary isotope effect is observed at the upper left corners of both the figures due to the coupling of C–D and methyl group rotation (see Fig. 5b).

4.2 Vibrational frequencies of anti-o-DMB

For the deuterated species, the overall RMSD shows a similar behavior as in undeuterated MB. Calculated harmonic and anharmonic diagonal frequencies are quite offset from the reference frequencies, which gives high RMSD values of 137 cm^{-1} and 130 cm^{-1}, respectively. Non-correlated VSCF dual level frequency calculations based on MP2/aug-cc-pVTZ diagonal and PM3 pair potentials also deviate considerably from the reference frequencies (RMSD = 76 cm^{-1}). The non-correlated VSCF frequencies employing DF-MP2/cc-pVDZ pair and DF-MP2/aug-cc-pVTZ diagonal potentials show good agreement with the reference frequencies and yield a very low RMSD of 14 cm^{-1}, for all 48 modes. Figs. 8a, 8b and 8c depict the general features of the different computational methods for the deuterated MB. Table 2 presents the vibrational

frequencies for the anti-o-DMB. Dual level frequency calculation employing DF-MP2/aug-cc-pVTZ diagonal potentials and PM3 pair potentials for all 40 low frequency modes are not reliable, but for the high frequency modes it yields quite reasonable results. For the low frequency modes (40 modes) the non-correlated VSCF employing DF-MP2/aug-cc-pVTZ diagonal as well as DF-MP2/cc-pVDZ pair potentials are in good agreement with the reference frequencies, yielding a RMSD of 13 cm^{-1}. This level of computation is also adequate for the high frequency region and yields a RMSD for the 8 C–H stretch vibrational modes of 17 cm^{-1}.

4.3 C–D band

The harmonic C–D vibrational frequencies at DF-MP2/aug-cc-pVTZ level are rather large, they are 2384 cm^{-1} and 2392 cm^{-1} for the syn- and anti-o-DMB, respectively. The anharmonic diagonal frequency calculation at DF-MP2/aug-cc-pVTZ level improve the results over harmonic calculation by about 70 cm^{-1}. It is noteworthy that the C–D stretching frequency is significantly improved by using the pair potentials calculated at DF-MP2/cc-pVDZ level. The non-correlated dual level VSCF method yields C–D vibrational frequencies of 2171 cm^{-1} and 2161 cm^{-1}, for the two isotopomers.

Table 3 The C–D vibrational frequency for anti-o-DMB. The diagonal potential for the C–D stretch vibrational mode is calculated at different level of theory and employing different size of basis sets. All other diagonal and pair coupling potentials are calculated at DF-MP2/cc-pVDZ level.

isotope	Method	Basis	Diag.	SCF	V-MP2	VC-MP2
	MP2	DZ	2367	2233	2243	2247
syn-o	MP2	TZ	2336	2187	2210	2210
DMB	MP2	ATZ	2198	2180	2202	2201
	CCSD(T)	TZ	2308	2161	2185	2184
	MP2	DZ	2374	2242	2257	2257
	MP2	TZ	2343	2196	2220	2219
	MP2	QZ	2338	2190	2214	2214
	MP2	ADZ	2359	2221	2239	2239
anti-o	MP2	ATZ	2235	2189	2212	2212
DMB	MP2	AQZ	2335	2188	2212	2211
	Ext	AVXZ	2331	2183	2208	2207
	CCSD(T)	TZ	2315	2171	2194	2194
	CCSD(T)	T/QZ	2310	2166	2190	2189
	PM3	selected triple		2172	2197	2197

An interesting result is observed when the dual level calculations are performed with systematically improved diagonal PES for the C–D stretch vibrational mode. With the improved basis set (for all atoms same basis sets are used) for the diagonal PES, the C–D anharmonic vibrational frequency exhibits a red shift. The frequency change is rather large for the DZ to TZ basis sets, and it converges quickly for larger basis sets. For example, when the diagonal potential for C–D (in anti-o-DMB) vibrational mode is calculated with augmented basis sets, a 32 cm^{-1} frequency shift is observed going from AVDZ to AVTZ. On the other hand, a basis set improvement from AVTZ to AVQZ shows just 1 cm^{-1} frequency shift (Table 3 coloumn SCF). The C–D shows also a red shift when highly correlated methods are used. A non-correlated VSCF calculation where the diagonal potential for the C–D vibrational mode is calculated at the DF-L-CCSD(T)/cc-pVTZ level, yields C–D frequencies of 2161 cm^{-1} and 2171 cm^{-1} for the syn- and anti-o-DMB respectively. When the DF-L-CCSD(T) calculation is performed using cc-pVQZ basis only for the deuterium and the directly connected carbon (for all other atoms cc-pVTZ basis are used), the frequency is lowered further by 5 cm^{-1} with respect to the DF-L-CCSD(T)/cc-pVTZ result (Table 3).

A detailed analysis of the coupling pattern shows that only a few modes are coupled with the C–D stretch vibrational mode. It is observed that modes 17 and 19 which correspond to the C–D bending modes, are strongly coupled with the C–D stretching mode. The other modes like 12, 13, 14, 15, 16, 18, 21, 24, have some weak coupling with the C–D stretch vibrational mode (see supplemental information). All these modes are involved with some kind of C–D bending motions (see Table 2).

One might expect that higher order terms in the many-body expansion of the PES have a significant influence on the vibrational frequency of the anharmonic system. The PM3 triple coupling potentials were used for such an analysis. Selected PM3 level triple couplings were added to the DF-MP2/cc-pVDZ pair coupling. This lowers the C–D stretching frequency negligibly (see supplemental information) indicating a minor influence of triple couplings[55] for this particular mode.

Two significant peaks are observed in the linear IR absorption spectra (see lower right magnified region in Fig. 3) which are equally separated from the calculated C–D stretch frequency at 2189 cm^{-1}. It seems that the C–D vibrational stretching mode is coupled with some low vibrational modes and due to the Fermi resonance it split up into two bands.

4.4 C=O band

Due to the structural arrangement, there is a possibility to form a strained five membered ring between the ester and the phenyl ring, which may induce an additional coupling between the C=O and the C–D band. The possible structure is shown in Fig. 6c. Both the oxygen atoms in the ester group may take part in five membered rings along with the ortho and β-hydrogens of the phenyl ring. The calculated possible non-bounded distances are 2.499 Å and 2.397 Å for the syn- and anti- positions, respectively, which are much larger than the required bond length to form a true five membered ring. There-

Table 4 Dual level VSCF anharmonic vibrational frequency for the C=O stretch mode with DF-L-CCSD(T)/cc-pVTZ diagonal and DF-MP2/cc-pVDZ pair potentials.

Isotope	SCF	V-MP2	VC-MP2	Experimental
syn-o-DMB	1724.5	1724.4	1724.5	
anti-o-DMB	1724.3	1724.1	1724.1	1724
MB	1725.6	1727.2	1727.2	

fore, isotopic substitution at the ortho position in the phenyl ring does not have any influence on the C=O vibrational frequency. The C=O vibrational frequency remains largely unchanged for both syn- and anti-o-DMB (see Table 4). Anharmonic frequencies in dual level calculations yield the same frequency of $1724\,cm^{-1}$ for both syn- and anti- conformers, which is in agreements with the experimental results.

4.5 Anharmonicity observed in the VSCF calculations

Table 5 Diagonal anharmonicity for vibrational frequencies of MB and its two isotopomers are calculated at the non-correlated VSCF method.

Mode	Isotopomer			Mode	Isotopomer		
No.	MB	syn-	anti-	No.	MB	syn-	anti-
1	17.7	18.9	17.6	25	13.9	13.2	12.2
2	17.5	16.8	16.7	26	9.7	5.7	1.3
3	83.8	78.2	79.4	27	10.4	10.3	9.9
4	4.2	4.1	3.8	28	22.9	22.9	19.7
5	9.1	8.9	8.8	29	5.6	6.2	5.9
6	3.8	3.8	3.7	30	-3.2	-8.3	-6.3
7	-5.7	-2.5	-2.2	31	4.9	7.2	4.5
8	3.7	4.4	3.6	32	1.5	10.9	9.9
9	5.2	5.8	5.3	33	5.0	4.2	6.7
10	0.3	0.7	0.8	34	3.8	6.2	5.2
11	1.9	1.9	1.9	35	1.2	0.9	1.2
12	-0.5	-0.9	-1.3	36	-10.2	-10.1	-10.1
13	21.1	21.7	19.6	37	2.9	3.4	2.4
14	15.0	14.9	15.5	38	-2.1	-1.3	-1.9
15	1.3	-0.1	0.3	39	0.0	0.9	0.3
16	7.8	7.0	5.5	40	-6.8	-7.1	-6.6
17	25.7	4.0	3.7	41	-120.8	-28.7	-29.1
18	1.6	9.6	9.9	42	-278.7	-214.3	-216.9
19	11.4	12.6	15.0	43	-155.0	-123.6	-123.7
20	3.3	-5.1	-5.9	44	-198.7	-170.1	-124.9
21	26.0	29.6	24.4	45	-88.5	-114.6	-68.5
22	5.7	1.7	3.4	46	-102.3	-90.3	-87.4
23	21.1	20.4	21.5	47	-88.3	-87.4	-85.1
24	-2.1	0.1	4.4	48	-67.7	-70.3	-94.5

The diagonal anharmonicities in frequency calculations are presented in Table 5 where mode numbers are based on the harmonic normal mode analysis. The diagonal anharmonicities are very high for the high frequency C–H stretch vibrational modes, up to a few hundred wavenumbers. Especially mode 42, which is unexpectedly red shifted, shows maximum anharmonicity. Other than the C–H stretch vibrational modes, diagonal anharmonicities are rather small ($< 10\,cm^{-1}$). Few low frequency modes show anharmonicities slightly higher than $10\,cm^{-1}$. These vibrational modes are mostly involved with C–H bending motions (see Table 2). For the first three modes the calculated vibrational frequencies are not reliable and for that reason anharmonicities are also unreliable.

4.6 Off-diagonal anharmonicity

Off-diagonal anharmonicities calculated for the few spectroscopically most important modes are presented in Table. 6. Calculated off-diagonal anharmonicities for the C=O vs. C–D

Table 6 Off diagonal anharmonicities for the C=O and C–D coupling modes calculated with non-correlated VSCF method with DF-MP2/AVTZ diagonal and DF-MP2/VDZ pair potentials.

Coupling	level	ω_a	ω_b	ω'	$\Delta\omega$
CO CD_7	SCF	1771.03	2233.49	4003.846	0.67
	V-MP2	1768.81	2242.75	4012.076	-0.52
	VC-MP2	1768.81	2246.59	4015.142	0.36
CO CD_{11}	SCF	1770.62	2242.33	4012.771	0.18
	V-MP2	1768.75	2257.22	4025.613	0.36
	VC-MP2	1768.75	2257.22	4025.654	0.32

coupling modes for both the isotopomers are less than a wave number. Such a negligibly small off-diagonal anharmonicity also indicates that there is negligible direct coupling between the C=O and the C–D vibrational modes.

5 Conclusions

It has been observed that harmonic frequencies are very poor approximation to assign the vibrational frequencies of Methyl benzoat and its two isotopomers. Anharmonic diagonal frequencies show some improvements but were still not sufficient to reach a reasonable assignment. The fundamental transition frequencies calculated with the VSCF method from a pair potential energy surface expansion seem promising, especially when the 2D PES are calculated at a sufficiently high ab initio level. The success of the VSCF frequency calculations depends upon the accuracy of the PES, in particular near the equilibrium where denser grid points are required. Dual level computations in which the diagonal anharmonic potential along a single vibrational mode is calculated using higher level ab initio methods than for coupling potentials provide an efficient route to the computation of the PES expansion in the VSCF framework. Such a dual level VSCF

calculation with DF-L-CCSD(T)/cc-pVTZ diagonal and DF-MP2/cc-pVDZ pair coupling potentials provided a nearly perfect agreement of the C=O vibrational frequency with respect to the experimental result.

Carrying out a systematic study, it has been shown that all pair couplings are not necessary to describe a particular vibrational band. Using only 14 coupling potentials for the C–D stretch vibrational mode the computed frequency is in good agreement with the result based on the full set of 1128 couplings. Non-uniform IMLS interpolation has been successfully used to reduce the computational cost for potential energy surface generation even further.

An unexpected red shift has been observed for a C–H stretch vibrational mode when the VSCF calculation has been performed with pair coupling potentials. The inability to find this mode in harmonic and diagonal anharmonic calculations indicates that this is a concerted anharmonic effect, pair and higher order couplings are in fact necessary to understand this feature. The investigations for the C–H(D) stretch vibrational modes with selected triple couplings at PM3 level do not improve the results much over the ab initio pair coupling calculations. This could indicate that either PM3 triple coupling potentials are in sufficient or that higher order coupling effects are negligible in this model.

The correct assignment of the C–D stretch frequency still poses a problem to both the theoretician and experimentalist. The calculated C–D stretch frequency just sits between the two strong peaks observed in the linear IR absorption spectra at the expected C–D frequency region. It seems that the C–D stretch frequency mode is coupled with some low vibrational frequency modes and thus it is shifted equally in both directions and appears as two peaks. Vibrational CI calculation may be necessary to describe this feature.

The diagonal and the off-diagonal anharmonicities have been calculated by non-correlated VSCF method. Other than for a few low frequency modes, which are involved in the C–H bending modes, diagonal anharmonicities are very small. The negligible off-diagonal anharmonicity for C=O and C–D coupling modes indicates that these modes are mostly decoupled.

VSCF is a mean field approach. Calculation of combination band and degenerate or near degenerate vibrational modes are still a problem with VSCF approach. For degenerate vibrational modes it causes singularities, as a result calculation is collapsed. To overcome this problem for combination band and near degenerate vibrational mode, it is necessary to calculate both the vibrational bands separately or treat them using CI calculation.

6 Acknowledgments

I would like to thank Christoph Scheurer for his continuous support to carry on this project. This work has been supported by Deutsche Forschungsgemeinschaft. Computational facility from Leibniz-Rechenzentrum is gratefully acknowledged.

References

1 *Ultrafast Infrared Vibrational Spectroscopy*, ed. M. D. Fayer, CRC Press, New York and London, 2013.
2 P. J. Stephens, *J. Phys. Chem.*, 1985, **89**, 748–752.
3 D. J. Minick, R. C. B. Copley, J. R. Szewczyk, R. D. Rutkowske and L. A. Miller, *Chirality*, 2007, **19**, 731–740.
4 L. Barron and A. Buckingham, *Mol. Phys.*, 1971, **20**, 1111–1119.
5 J. Haesler, I. Schindelholz, E. Riguet, C. G. Bochet and W. Hug, *Nature*, 2007, **446**, 526–529.
6 J. Šebestík and P. Bouř, *Angewandte Chemie Int. Ed.*, 2014, **53**, 9236–9239.
7 P. Hamm, M. Lim and R. M. Hochstrasser, *J. Phys. Chem. B*, 1998, **102**, 6123.
8 S. Borman, *Chem. Eng. News*, 2000, **78**, 41.
9 D. M. Jonas, *Annu. Rev. Phys. Chem.*, 2003, **54**, 425.
10 T. Brixner, J. Stenger, H. M. Vaswani, M. Cho, R. E. Blankenship and G. R. Fleming, *Nature*, 2005, **434**, 625.
11 J. Zheng, K. Kwak, J. Xie and M. D. Fayer, *Science*, 2006, **313**, 1951.
12 A. Tokmakoff, *Science*, 2007, **317**, 54.
13 C. Scheurer and S. Mukamel, *J. Chem. Phys.*, 2001, **115**, 4989.
14 C. Scheurer and S. Mukamel, *J. Chem. Phys.*, 2002, **116**, 6803.
15 R. M. Hochstrasser, *Proc. Nat. Acad. Sci.*, 2007, **104**, 14190–14196.
16 C. Scheurer and T. Steinel, *ChemPhysChem*, 2007, **8**, 503.
17 J. Wang and R. M. Hochstrasser, *J. Phys. Chem. B*, 2006, **110**, 3798.
18 R. B. Gerber, B. Brauer, S. K. Gregurick and G. M. Chaban, *Phys. Chem. Comm.*, 2002, **21**, 142.
19 M. Bounouar and C. Scheurer, *Chem. Phys.*, 2006, **323**, 87.
20 K. S. Maiti and C. Scheurer, *J. Chem. Chem. Eng.*, 2013, **7**, 1100.
21 Z. Bačíc, R. B. Gerber and M. A. Ratner, *J. Phys. Chem.*, 1986, **90**, 3606.
22 J. R. Henderson, J. Tennyson and B. T. Sutcliffe, *J. Chem. Phys.*, 1993, **98**, 7191.
23 N. J. Wright and J. M. Hutson, *J. Chem. Phys.*, 1999, **110**, 902.
24 J. B. Anderson, *J. Chem. Phys.*, 1975, **63**, 1499.
25 V. Buch, *J. Chem. Phys.*, 1992, **97**, 726.
26 R. N. Barnett and K. B. Whaley, *J. Chem. Phys.*, 1993, **99**, 9730.
27 V. Barone, J. Bloino, M. Biczysko and F. Santoro, *J. Chem. Theo. Comput.*, 2009, **5**, 540–554.
28 D. Strobusch and C. Scheurer, *J. Chem. Phys.*, 2011, **135**, –.
29 J. Hudecová, V. Profant, P. Novotná, V. Baumruk, M. Urbanová and P. Bouř, *J. Chem. Theo. Comput.*, 2013, **9**, 3096–3108.
30 J. M. Bowman, *J. Chem. Phys.*, 1978, **68**, 608.
31 R. B. Gerber and M. A. Ratner, *Chem. Phys. Lett.*, 1979, **68**, 195.
32 R. B. Gerber and M. A. Ratner, *Adv. Chem. Phys.*, 1988, **70**, 97.
33 J. O. Jung and R. B. Gerber, *J. Chem. Phys.*, 1996, **105**, 10332.
34 A. Barth and C. Zscherp, *Quarterly Reviews of Biophysics*, 2002, **35**, 369.
35 K. S. Maiti, A. Samsonyuk, C. Scheurer and T. Steinel, *Phys. Chem. Chem. Phys.*, 2012, **14**, 16294.
36 C. Møller and M. S. Plesset, *Phys. Rev.*, 1934, **46**, 618.
37 M. S. Gordon, J. A. Pople and M. J. Frisch, *Chem. Phys. Lett.*, 1988, **153**, 503.
38 M. J. Frisch, M. S. Gordon and J. A. Pople, *Chem. Phys. Lett.*, 1990, **166**, 275.
39 H.-J. Werner, P. J. Knowles *et al.*, *MOLPRO 2002.6, a package of ab initio programs*, 2003, see http://www.molpro.net.
40 M. Schütz and H. J. Werner, *Chem. Phys. Lett.*, 2000, **318**, 370.
41 M. Schütz, *Phys. Chem. Chem. Phys*, 2002, **4**, 3941.

42 M. Schütz and F. R. Manby, *Phys. Chem. Chem. Phys.*, 2003, **5**, 3349.
43 S. Grimme, *J. Chem. Phys.*, 2003, **118**, 9095.
44 S. Carter, J. M. Bowman and L. B. Harding, *Spectrochim. Acta A*, 1997, **53**, 1179.
45 C. d. Boor, *A Practical Guide to Splines, Berlin*, Springer (1st Ed.), 1978.
46 Lancaster and Salkauskas, *Curve and Surface fitting*, Acad. Press, 1987.
47 S. Chattopadhyay, *Indian J. Physics*, 1968, **42**, 335.
48 J. H. S. Green and D. J. Harrison, *Spec. Act.*, 1977, **33A**, 583.
49 E. B. Wilson, *Phys. Rev.*, 1934, **45**, 706.
50 D. H. Whiffen, *J. Chem. Soc.*, 1956, 1350.
51 P. Lemman, *Private communication*.
52 S. D. for Organic Compounds.
53 T. Steinel, *Private communication*.
54 J. S. Rollett and J. H. Wilkinson, *Comp. J.*, 1961, **4**, 177.
55 G. Rauhut, *J. Chem. Phys.*, 2004, **121**, 9313.